

Received August 28, 2019; reviewed; accepted November 13, 2019

## Leaching kinetics of iron from coal-series kaolin by oxalic acid solutions

Hui Shao <sup>1,2</sup>, Mengjiao Ji <sup>2</sup>, Mingming Yu <sup>1</sup>

<sup>1</sup> School of Resources and Environmental Engineering, Jiangxi University of Science and Technology, Ganzhou 341000, China

<sup>2</sup> Hainan Branch, China Triumph International Engineering Co, Ltd, Haikou 570125, China

Corresponding author: [mingmy1990@163.com](mailto:mingmy1990@163.com) (Mingming Yu)

**Abstract:** Removal of iron from coal-series kaolinite and its kinetics by chemical leaching were investigated in this paper. The optimal removal rate of iron reaches 29.09% (the content of Fe<sub>2</sub>O<sub>3</sub> decreased from 0.55 to 0.39%) under the conditions of 100 °C, 0.4 M C<sub>2</sub>H<sub>2</sub>O<sub>4</sub>, and liquid-to-solid ratio of 4 cm<sup>3</sup>/g for 120 min. The leaching process was successfully described by the Avrami model and mainly controlled by internal diffusion control of shrinking core model, the apparent activation energy is 18.46 kJ/mol. The experimental results were consistent with the internal diffusion control of shrinking core model, improving acid concentration and leaching temperature could promote the removal of iron from coal-series kaolin.

**Keywords:** coal-series kaolin, leaching kinetics, iron removal rate, oxalic acid

### 1. Introduction

Considering the numerous usage in ceramics, paper, paints, fiberglass, inks, pharmaceuticals, and cement, kaolin have gained a growing demand (Huang et al., 2019), and the high-quality kaolin has almost been exhausted; thus, exploiting coal-measure kaolin has become increasingly important.

Coal-series kaolin, as a by-product of seam deposition in coal accumulating basins, has large reserves (about 3.8 billion tonnes in China) (Querol et al., 2008). Coal-series kaolin has high purity, which contains almost no feldspar and quartz. But the iron content is higher, which not only affects the whiteness, but also affects its application. It is difficult to meet the industrial requirements by conventional iron removal process, as iron impurity is mainly fine-grained dissemination (Zhu et al., 2014).

Several chemical methods including bioleaching treatment and acid leaching were applied to kaolin beneficiation in order to removing Fe and other associated impurities. Using bioleaching, the content of Fe<sub>2</sub>O<sub>3</sub> could decrease from 0.94 to 0.46%, while the whiteness increased from 61 to 82% after 10 days' treatment with dissimilatory Fe(III)-reducing bacteria (DIRB). But the leaching time is too long for bioleaching treatment, so it is difficult to achieve industrialization (Guo et al., 2010).

By acid leaching at 100 °C with 0.15 M oxalic acid and 90 min reaction time, the brightness could up to 80% (Veglio et al., 1993; Ambikadevi and Lalithambika, 2000). Xia et al. (2012) studied a bleaching process of a kaolinite using thiourea as the leachant agent in the iron removal process, in the absence and presence of ultrasound. The optimum conditions for the maximum whiteness of 89% with ultrasound were determined (Xia et al., 2012)

Zhu et al. detected that nearly all of the structural ferrous ions in coal-series kaolin were removed by hydrochloric acid, but it is difficult to remove the structural ferric ions and ferric oxides evolved from the structural ferrous ions using calcination. Thus, iron removal by acids should be conducted prior to calcination (Zhu et al., 2014). For acid leaching, heterogeneous fluid-solid reactions are involved and various acid leaching kinetic models were studied. It is thought that the kinetic data for the extraction

of iron from kaolin are very important for industrial applications such as raw material for the paper and ceramic industries (Martínez-Luévanos et al., 2011).

Leaching kinetic studies of Al from coal-series kaolin were carried out in recent years (Lin et al., 2018). The types of chemical reactions of impurities in acid are different because of the difference in character of particles, the type of phases, so the leaching kinetics of all the elements may not exactly follow the same pattern. There has been no report on the leaching kinetics of Fe from coal-series kaolin so far. Thus, the objective of this study is to remove iron from coal-series kaolin by acid leaching. By comparing the leaching effects of different acids, a suitable acid was found, which can remove iron from coal-series kaolin but has little influences on destroying crystal structure of kaolinite. The leaching kinetics of iron from coal-series kaolin and the apparent activation energy are determined.

## 2. Materials and methods

### 2.1. Materials

The raw materials used in this study were the concentrates of coal-series kaolin after magnetic separation-flotation process. The composition of the raw materials was analysed by X-ray fluorescence and shown in Table 1. The results indicate the sample consisted mainly of 35.82% alumina, 48.22% silicon dioxide and 0.55% iron oxide.

Table 1. Chemical compositions of the sample (mass fraction, %).

Composition	SiO <sub>2</sub>	Al <sub>2</sub> O <sub>3</sub>	Fe <sub>2</sub> O <sub>3</sub>	SO <sub>3</sub>	TiO <sub>2</sub>	CaO	Na <sub>2</sub> O	P <sub>2</sub> O <sub>5</sub>	K <sub>2</sub> O	LOI
Content (wt%)	48.22	35.82	0.55	0.44	1.03	0.105	0.078	0.12	0.25	13.22

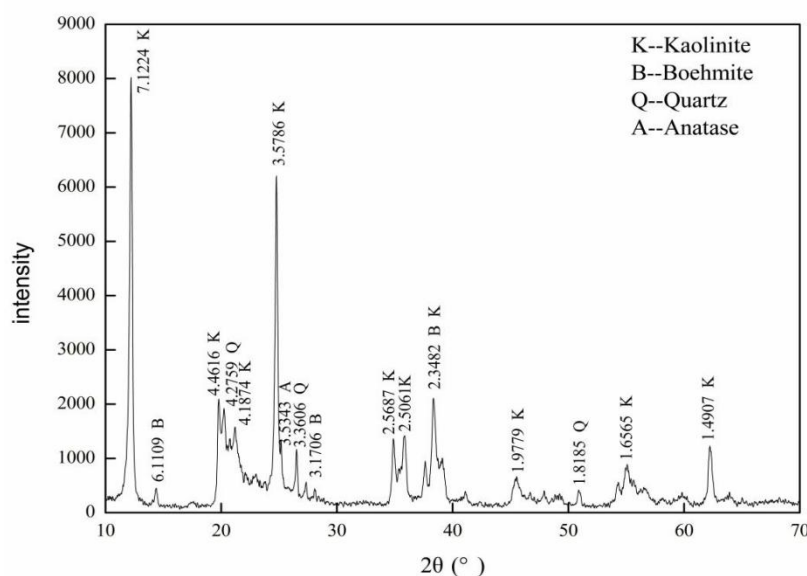


Fig. 1. X-ray diffraction patterns of coal-series kaolin

Fig. 1 shows the X-ray diffraction (XRD) pattern of the concentrates of coal-series kaolin after magnetic separation-flotation processes. It can be seen that the main crystalline phases are kaolinite (PDF card 79-1570), quartz (PDF card 33-0271), boehmite (PDF card 05-0355) and anatase (PDF card 21-1276). Iron oxides were not detectable due to low concentration in the kaolin.

### 2.2. Leaching tests

The leaching experiment was carried out in a three necked round bottom flask which was placed on a water bath (set at desired temperature). A sample of 10 g of the raw materials was transferred to flask containing the desired concentration of the acid maintained at a preset temperature. The slurry was

stirred with a magnetic needle at 600 rpm for the entire duration of the leaching, the leaching reaction was shown in equation 1 (Eq. 1). The effect of acid concentration, temperature, liquid/solid ratio and reaction time was investigated using sulphuric, hydrochloric and oxalic acid solutions respectively. During leaching experiments one of the parameters was varied while other parameters were maintained constant. At the end of the leaching, the slurry was filtered, water-washed and oven-dried. All the solutions generated in the leaching were analysed by (ICP-OES), and residues were characterized by SEM and XRF analysis. The removal percentage rate of iron removal was calculated using Eq. 2.



$$X = (\alpha/\beta) \times 100\% \quad (2)$$

where X is the removal rate percentage of Fe,  $\alpha$  is the content of Fe in the leaching solutions (ICP-OES), and  $\beta$  is the content of Fe in the raw coal-series kaolin.

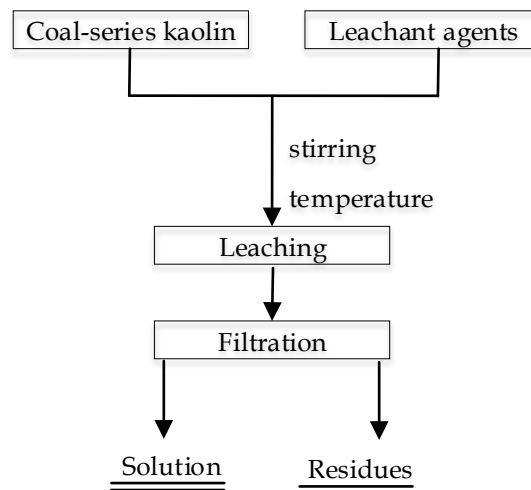


Fig. 2. The flow-sheet of leaching process

### 2.3. Reagents and equipment

X-ray fluorescence analysis (XRF) was conducted using an AXIOS system (PANalytical.B.V, Co., Ltd, Ea Almelo, Netherlands), and X-ray diffraction (XRD) analysis was measured with an RU-200B (Rigaku Co., Ltd, Tokyo, Japan). The pH meter used was a HM-40V (TOA Denpa Togyo, Co., Ltd, Tokyo, Japan). Prodigy 7 (Leeman Labs INC. Hudson, New Hampshire, USA) was used to conduct the Inductively Coupled Plasma Optical Emission Spectrometer (ICP-OES) analysis. Scanning Electron Microscope/Energy Dispersive Spectroscopy (SEM-EDS) analysis was carried out on a Zeiss Ultra Plus" (Carl Zeiss AG, Oberkochen, Germany). To compare color changes in the kaolin samples before and after leaching, the whiteness index of the samples was measured using a colorimeter (YQ-Z-48A, Hangzhou, China).

As for acid leaching process, sulfuric acid ( $\text{H}_2\text{SO}_4$ ), hydrochloric acid (HCl) and oxalic acid ( $\text{C}_2\text{H}_2\text{O}_4$ ) were used as the leachant agents. All chemicals were first grade reagents and deionized water was used for the preparation of all aqueous solutions.

## 3. Results and discussion

### 3.1. Effect of acid concentrations on iron removal rate of different acids

Leaching processes was conducted using hydrochloric acid, sulfuric acid and oxalic acid, respectively. In order to observe the effect of the concentration on iron removal rate, the experimental parameters considered were: reaction temperature = 80 °C, L/S = 4 cm<sup>3</sup>/g, reaction time = 90 min,  $[\text{H}_2\text{SO}_4] = 1.87\text{-}5.62$  M,  $[\text{HCl}] = 1.15\text{-}3.46$  M,  $[\text{C}_2\text{H}_2\text{O}_4] = 0.2\text{-}0.5$  M.

As shown in Figs. 3-5, the acid concentration played an important role in the leaching process. The Fe removal increased with increasing acid concentration within a certain range. Further increase of the acid concentrations, the Fe removal had a significant decrease. It indicates that increasing acid concen-

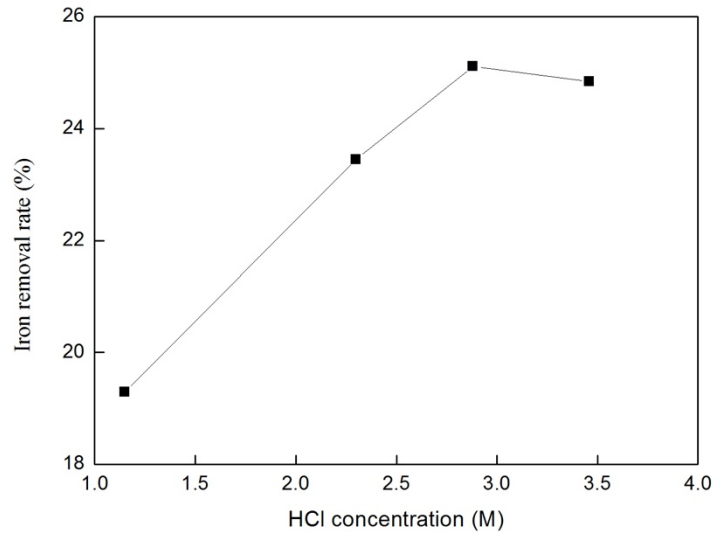


Fig. 3. Effect of HCl concentration on the iron removal rate of coal-series kaolin

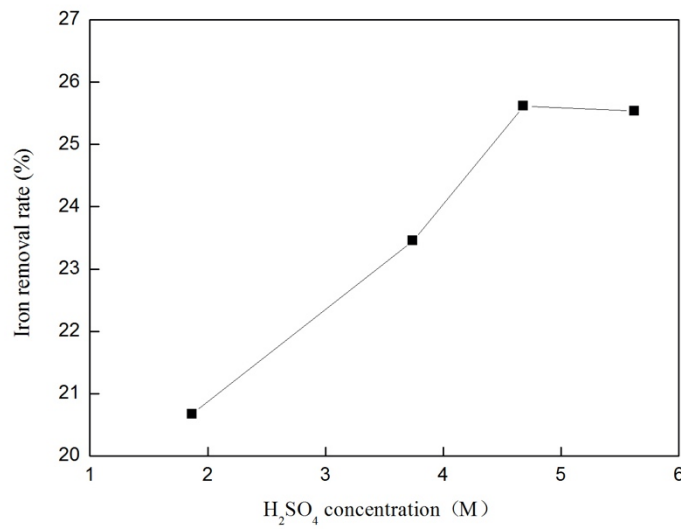


Fig. 4. Effect of H<sub>2</sub>SO<sub>4</sub> concentration on the iron removal rate of coal-series kaolin

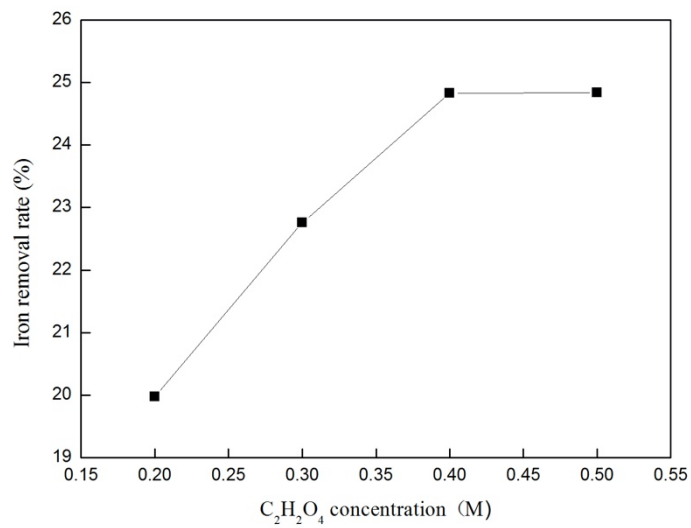


Fig. 5. Effect of C<sub>2</sub>H<sub>2</sub>O<sub>4</sub> concentration on the iron removal rate of coal-series kaolin

tration can promote leaching process, but excess hydrochloric acid could reduce the activity of  $H^+$  in acid solution, and is even not propitious to leach Fe from calcined kaolin (Lin et al., 2018). The optimum acid concentration for Fe removal of HCl,  $H_2SO_4$  and  $C_2H_2O_4$  was 2.88, 4.68 and 0.4 M, and the Fe removal was 25.6, 26.7 and 25.2%, respectively.

Table 2. The results of leaching rate of Al and iron

Acid	Al %	iron %
hydrochloric acid	7.70	25.11
sulfuric acid	12.68	25.62
oxalic acid	3.76	24.84

The leaching rate of Al and Fe on the optimum acid concentration of different acids was shown in Table 2. The results shown that the iron removal rate of iron has no significant difference, but the leaching rate of Al was 7.70, 12.68 and 3.76% using HCl,  $H_2SO_4$  and  $C_2H_2O_4$ , respectively. The leaching rate of Al was maximal using  $H_2SO_4$  and minimum using  $C_2H_2O_4$ , the results indicated that  $C_2H_2O_4$  could protect the kaolin structure compared with HCl and  $H_2SO_4$  (Martínez-Luévanos et al., 2011).

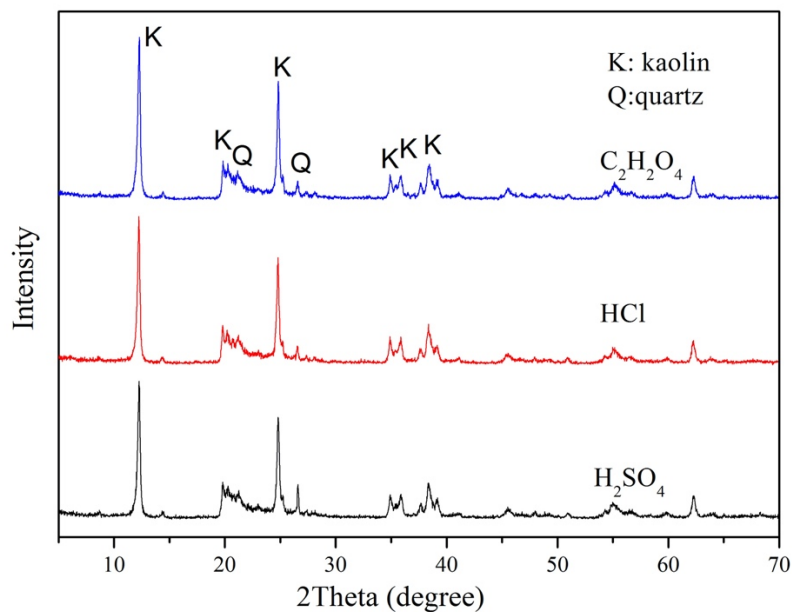


Fig. 6. XRD spectrum of acid leaching concentration

The XRD patterns for the phase analysis of residues generated during leaching process using different acid are shown in Fig. 6, which exhibit reduction in the peaks of kaolin (PDF card 79-1570). The kaolin peaks of residues using  $C_2H_2O_4$  as leachant was the highest, followed by  $H_2SO_4$  and HCl, indicating that the sulfuric acid damages the structure of kaolin most seriously, while oxalic acid damages the structure of kaolin less. The result was consistent with that in Table 2. Thus, to protect the kaolin structure,  $C_2H_2O_4$  was chosen as the best acid for removing iron from coal-series kaolin, and the optimum acid concentration  $C_2H_2O_4$  was 0.4 M.

### 3.2. Effect of liquid/solid ratio on iron removal rate

The effect of L/S (2-6  $cm^3/g$ ) on iron removal rate was studied using 0.4 M  $C_2H_2O_4$  at 80 °C for 90 min (Fig. 7). The results demonstrate that the iron removal rate increase with the increase of L/S from 2 to 4  $cm^3/g$ , which is attributed to the fact that at high L/S ratio, there are sufficient amount of  $C_2H_2O_4$  to react with the coal-series kaolin, and the increase of the L/S ratio decreases the viscosity of the slurry, favoring the mass transportation of the reactants in the system. For the L/S ratios of 4, the iron removal rate was 24.85%. Further, the increase of L/S ratios from 4 to 6 does not provide further improvement for the iron removal rate. Hence, 4  $cm^3/g$  was considered the optimum L/S for the experiments.

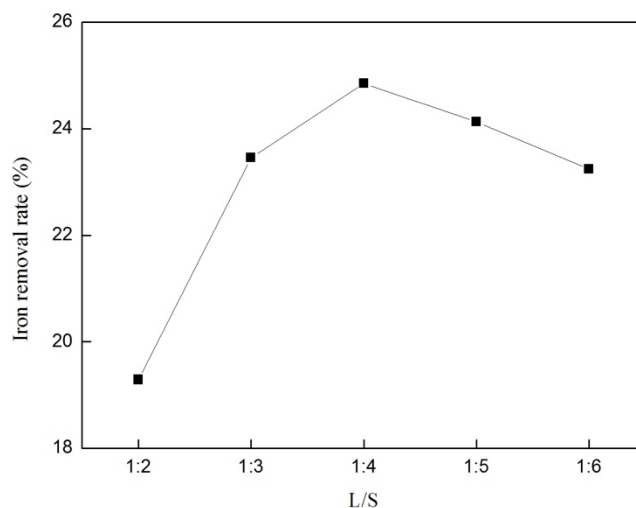


Fig. 7. Effect of liquid/solid ratio on the iron removal rate of coal-series kaolin

### 3.3. Effect of reaction time on iron removal rate

The reaction time of leaching is another important factor that influences the leaching process. The reaction time effect was examined in the range of 30-150 min under the conditions of 80 °C, 0.4 M  $C_2H_2O_4$ , and L/S of 4  $cm^3/g$ . As shown in Fig. 8, the iron removal rate was increased from 17.20 to 27.02% with an increase in the reaction time from 30 min to 120 min, and thereafter the removal rate was constant through 150 min. Hence, 120 min was considered the optimum time of leaching iron from coal-series kaolin.

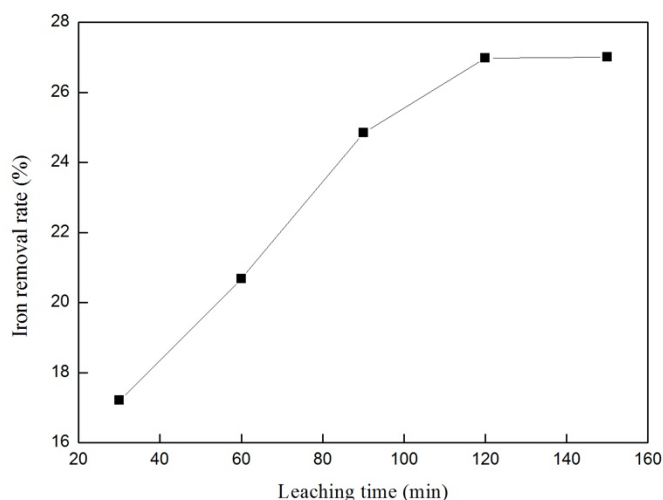


Fig. 8. Effect of reaction time on the iron removal rate of coal-series kaolin

### 3.4. Effect of temperature on iron removal rate

The effect of temperature on iron removal rate was studied using 0.4 M  $C_2H_2O_4$ , and L/S of 4  $cm^3/g$ , in the temperature range 25–100 °C for 120 min. The results indicate that high temperature promotes the removal of iron from coal-series kaolin (Fig. 9). The iron removal rate was increased from 18.59 to 29.09% with the increase of temperature from 25 to 100 °C. It indicates that high temperature can promote the diffusion of  $H^+$  in acid solution and further speed up the extraction of Fe. Thus 100 °C was chosen as the optimum temperature for leaching of iron from coal-series kaolin.

### 3.5. Discussion

The compositions of coal-series kaolin and residue after leaching using  $C_2H_2O_4$  were examined by XRF and SEM analyses. Compared with the coal-series kaolin (Table 1), the content of  $Fe_2O_3$  decreased from

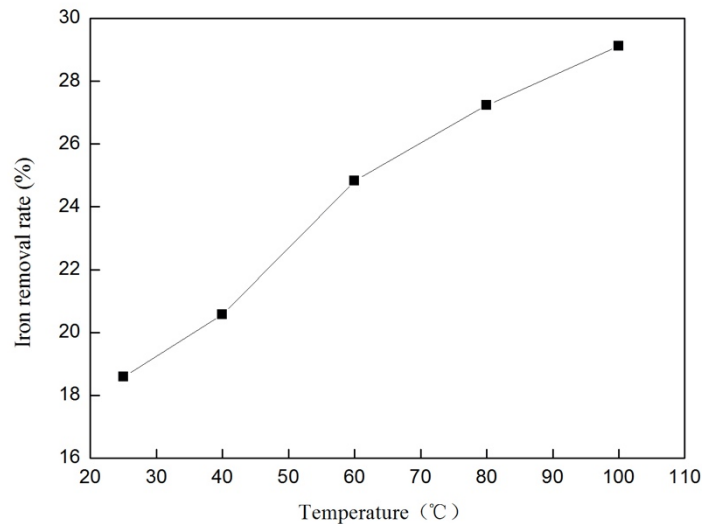


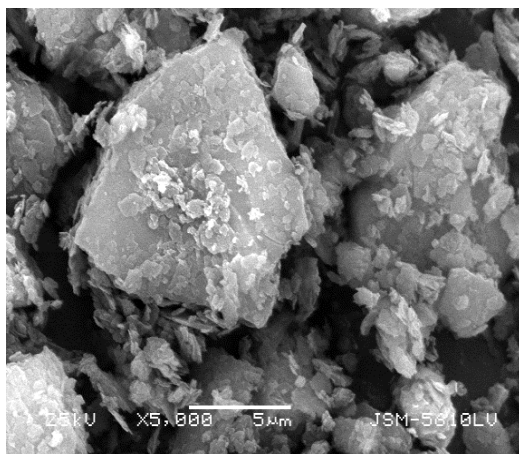
Fig. 9. Effect of temperature on the iron removal rate of coal-series kaolin

0.55 to 0.39%, the content of  $\text{SiO}_2$  and  $\text{Al}_2\text{O}_3$  has no obvious changes.

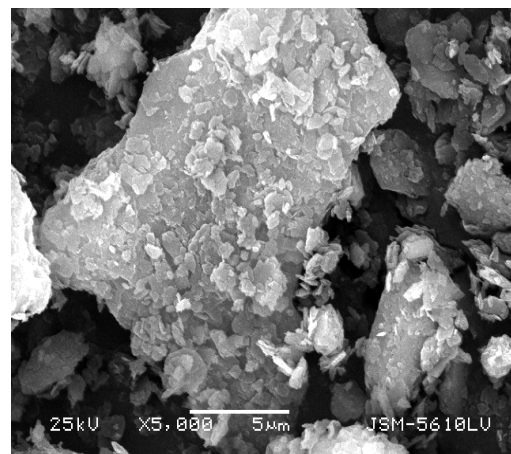
The SEM analysis of coal-series kaolin and the residue obtained from leaching process are shown in Fig. 10. The diagram shows that the particles of coal-series kaolin were irregular with small grains in the shape of scales. Compared with the coal-series kaolin, the diagram of residue shows that the looseness of the aggregate increased.

Table 3. XRF analysis for concentrate of acid leaching

Composition	$\text{SiO}_2$	$\text{Al}_2\text{O}_3$	$\text{Fe}_2\text{O}_3$	$\text{SO}_3$	$\text{TiO}_2$	$\text{CaO}$	$\text{Na}_2\text{O}$	$\text{P}_2\text{O}_5$	$\text{K}_2\text{O}$	LOI
Content (wt%)	48.74	34.44	0.39	0.23	1.16	0.104	0.089	0.039	0.244	14.28



(a) coal-series kaolin

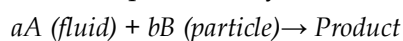


(b) leaching residue

Fig. 10. SEM images of coal-series kaolin and leaching residue

### 3.6 Kinetics analysis of removal rate of iron from coal-series kaolin

The leaching process of iron from coal-series kaolin using  $\text{C}_2\text{H}_2\text{O}_4$  solutions is a typical heterogeneous reaction in liquid–solid systems, the general form of a fluid–solid reaction is as follows:



In the reactions, the process rate is generally controlled by the slowest reaction, which can either be a chemical reaction at the surface, diffusion through the solid product (ash), or diffusion through the

fluid film. The controlling rate and the kinetic parameters for such reactions can be determined by integral analysis method (Levenspiel, 1972). For the non-catalytic reaction of particles surrounded by a fluid, the most commonly used models are discussed below:

(1) Shrinking core model:

The shrinking core model assumes that the rate may be controlled by a surface chemical reaction, diffusion through a fluid film (external diffusion of leached solute) or diffusion through the product layer (internal diffusion of leaching agent). Each of the reaction, film diffusion, and pore diffusion control mechanisms for the shrinking core model are discussed below. A detailed statistical study of heterogeneous, homogeneous and nucleation models for dissolution of waste concrete sample for mineral carbonation:

- Chemical reaction control (SC):

$$1-(1-X)^{1/3}=kt \quad (3)$$

- External diffusion control (SE):

$$1-(1-X)^{2/3}=kt \quad (4)$$

- Internal diffusion control (SI):

$$1-2/3X-(1-X)^{2/3}=kt \quad (5)$$

(2) Homogeneous models

In addition to the heterogeneous reaction models, the rate equations using pseudo homogeneous reaction models are also derived. In these models, fluid is assumed to be present evenly throughout the particle and reacts with solid surface everywhere. The rate equations for each of the above control mechanisms can be written as follows:

- Equation for the pseudo-homogeneous first order reaction (PF):

$$-\ln(1-X)=kt \quad (6)$$

- Equation for the pseudo-homogeneous second order reaction (PS):

$$(1-X)^{-1}-1=kt \quad (7)$$

(3) Avrami model

The Avrami model is derived originally from systems in which the crystallization phenomenon occurred and might be also used to derive the rate equations in non-catalytic fluid-solid systems (Tunc et al., 2007). The logarithmic form of Avrami model can be written as follows (AV):

$$\ln(-\ln(1-X)) = n \cdot \ln(t) + \ln(k) \quad (8)$$

### 3.6.1 Effect of oxalic acid concentration on removal rate of Fe

Effect of oxalic acid concentration on the removal rate of iron was studied at concentration up to 0.4 M, 80 °C, and the liquid/solid ratio was 4. As shown in Fig. 11, the removal rate of iron increases with increasing of oxalic acid concentration below 0.4 M and undulates above 0.4 M. It indicates that increasing acid concentration can increase the activity of H<sup>+</sup> in acid solution and promote leaching process, but excess oxalic acid is not propitious.

According to the experimental results in Fig. 10, fitting parameters for the different models are shown in Table 4 and Fig. 12., Fig. 13 shows a relationship between correlation coefficient (R<sup>2</sup>) and acid concentration. For homogeneous models, R<sup>2</sup> are decreased rapidly (R<sup>2</sup> ≤ 0.84) when the acid concentration is 0.3 M and the models are not suitable for describing the whole leaching process. In addition, for shrinking core model the R<sup>2</sup> of internal diffusion control are greatest especially at low acid concentration. It shows that the resistance to diffusion through the product layer controls the reaction rate. (Yu et al., 2017). In addition, the R<sup>2</sup> of Avrami model is always above 0.95. For Avrami model, when the values of n are ≤ 0.5 the reaction rate is diffusion controlled (Sokić et al., 2009). The value of n is below 0.5 with the acid concentration above 0.4 M, it indicates diffusion can be the primary obstruction for leaching iron from coal-series kaolin at high acid concentration.

In general, the experimental data fit to internal diffusion control and Avrami model. Compared with internal diffusion control model the R<sup>2</sup> of Avrami model is greater, the Avrami model is more suitable to deliver the leaching process.

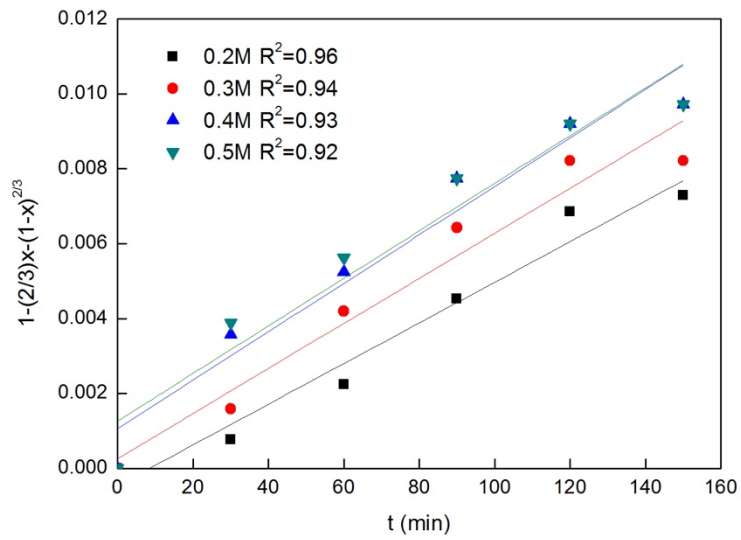


Fig. 11. The influences of acid concentration and leaching time on removal rate of iron with oxalic acid at 80 °C, at L/S=4

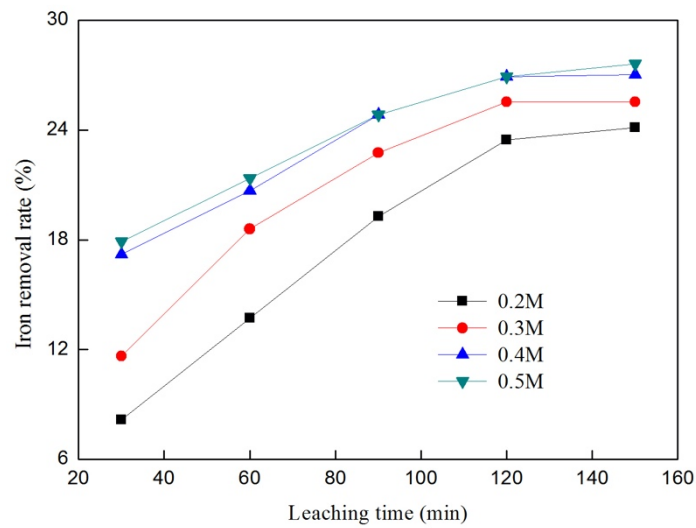


Fig. 12. Fitting curves of internal diffusion control of shrinking core model

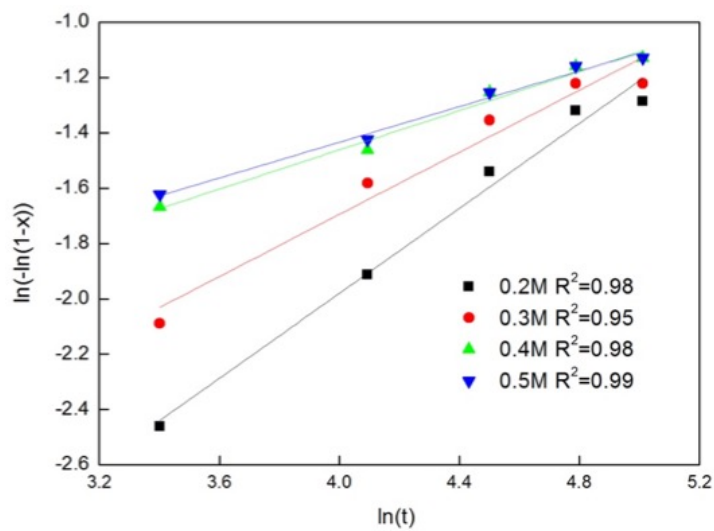


Fig. 13. Fitting curves of Avrami models

Table 4. Model parameters at different acid concentration

Model	concentration (M)		0.2	0.3	0.4	0.5
Shrinking core	$1-(2/3)X-(1-X)^{2/3}=kt$	$R^2$	0.96	0.94	0.93	0.92
		$k \cdot 10^5$	5.43	6.02	6.48	6.35
	$1-(1-X)^{2/3}=kt$	$R^2$	0.94	0.84	0.74	0.71
		$k \cdot 10^3$	1.15	1.16	1.15	1.13
	$1-(1-X)^{1/3}=kt$	$R^2$	0.95	0.85	0.76	0.73
		$k \cdot 10^4$	6.02	6.13	6.12	6.01
Pseudo homogeneous	$X=kt$	$R^2$	0.93	0.84	0.92	0.93
		$k \cdot 10^2$	13.9	11.6	9.03	8.33
	$-\ln(1-X)=kt$	$R^2$	0.94	0.85	0.93	0.93
		$k \cdot 10^3$	1.67	1.44	1.17	1.08
	$1/(1-X)=kt$	$R^2$	0.94	0.87	0.93	0.94
		$k \cdot 10^3$	2.02	1.79	1.52	1.41
Avrami	$\ln(-\ln(1-X))=n\ln(t)+\ln(k)$	$R^2$	0.98	0.95	0.98	0.99
		$n$	0.77	0.56	0.35	0.32
		$\ln k$	-5.05	-3.94	-2.88	-2.72

### 3.6.2. Effect of temperature on removal rate of Fe

Effect of temperature on the removal rate of iron was studied at 25-100 °C, respectively, with oxalic acid concentration of 0.4 M, when the L/S ratio was 4. As shown in Fig. 14, the removal rate of iron increases with increasing of temperature. It indicates that high temperature can promote the diffusion of  $H^+$  in acid solution and further speed up the extraction of Fe. In addition, it is important to note that the reaction rate is fast within 120 min and then slow at last. A possible explanation is that the reactions can reach equilibrium at the final stage of the reaction.

According to the experimental results in Fig. 14, fitting parameters for the different models are shown in Table 5 and Fig. 15. Fig. 17 shows a relationship between correlation coefficient ( $R^2$ ) and acid concentration. As shown in Table 5, for homogeneous models,  $R^2$  is decreased rapidly ( $R^2 \leq 0.89$ ) when the temperature is above 60 °C and the models are not suitable for describing the whole leaching process. For shrinking core model the  $R^2$  of internal diffusion control are greatest especially at high temperature. It shows that the resistance to diffusion through the product layer controls the reaction rate. In addition, the  $R^2$  of Avrami model is always above 0.93. The value of  $n$  are below 0.5 when the temperature is above 40 °C, it indicates diffusion can be the primary obstruction for leaching iron from coal-series kaolin when the temperature is above 40 °C.

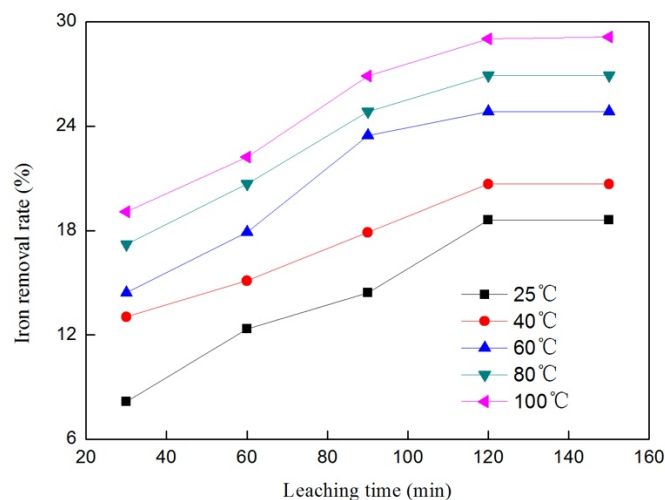


Fig. 14. The influences of leaching temperature and leaching time on removal rate of Fe with 0.4 M oxalic acid, at L/S=4

According to the data in Figs. 16 and 18, apparent activation energy of the leaching reaction was calculated according to the Arrhenius formula. The calculated apparent activation energies of the two models were 11.31 and 18.46 kJ/mol, respectively.

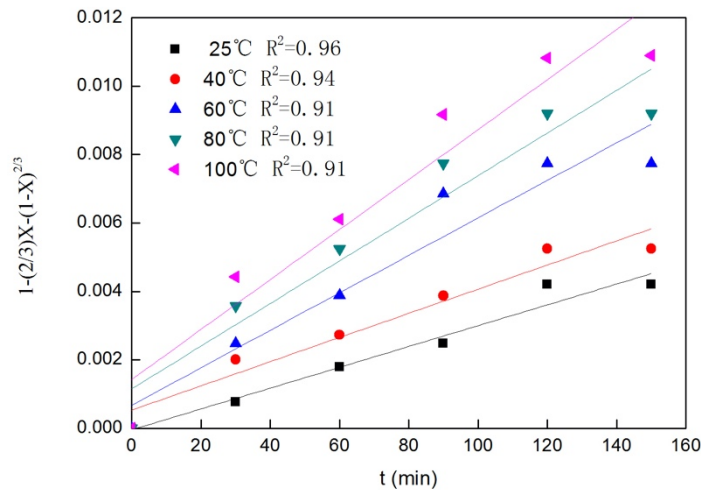


Fig. 15. Fitting curves of internal diffusion control of shrinking core model

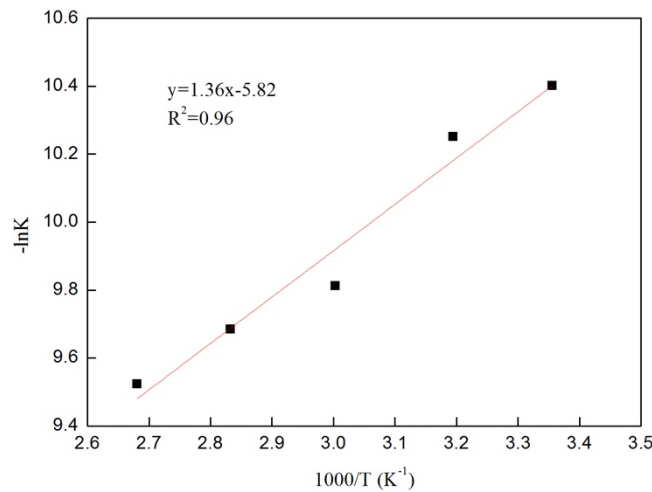


Fig. 16. Arrhenius plots of internal diffusion control of shrinking core model

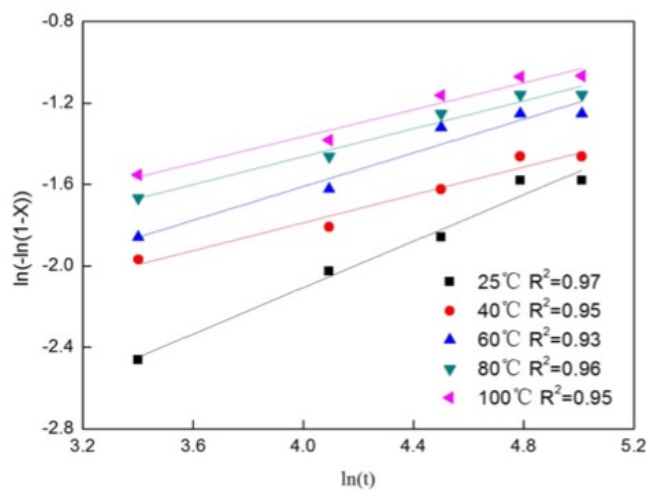


Fig. 17. Fitting curves of Avrami models

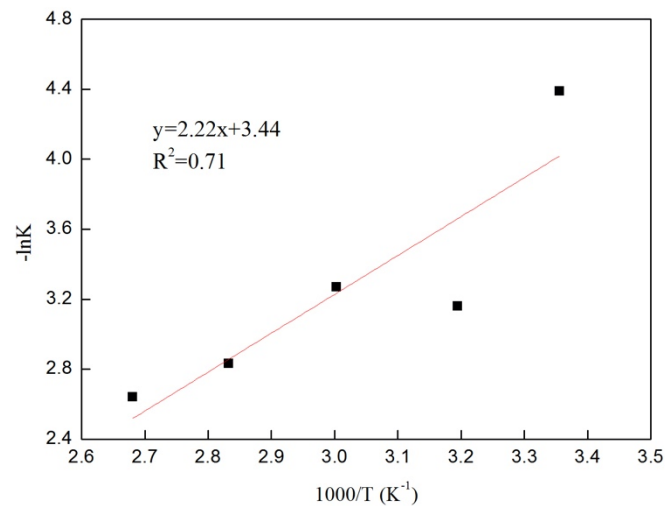


Fig. 18. Arrhenius plots of Avrami models

Table 5. Model parameters at different leaching temperature

Model	Leaching temperature (°C)		25	40	60	80	100
Shrinking core	$1-(2/3)X-(1-X)^{2/3}=kt$	$R^2$	0.96	0.94	0.91	0.91	0.91
		$k \cdot 10^5$	3.04	3.53	5.48	6.23	7.31
	$1-(1-X)^{2/3}=kt$	$R^2$	0.89	0.75	0.77	0.72	0.88
		$k \cdot 10^4$	8.32	8.55	10.8	11.3	6.56
	$1-(1-X)^{1/3}=kt$	$R^2$	0.89	0.76	0.78	0.74	0.89
		$k \cdot 10^4$	4.32	4.46	5.68	5.98	3.60
Pseudo homogenous	$X=kt$	$R^2$	0.92	0.93	0.83	0.88	0.88
		$k \cdot 10^2$	9.03	6.94	9.26	8.56	0.89
	$-\ln(1-X)=kt$	$R^2$	0.92	0.93	0.84	0.88	0.89
		$k \cdot 10^3$	1.05	0.84	1.18	1.11	1.19
	$1/(1-X)=kt$	$R^2$	0.92	0.93	0.84	0.89	0.89
		$k \cdot 10^3$	1.22	1.01	1.45	1.43	1.58
Avrami	$\ln(-\ln(1-X))=n \ln(t)+\ln(k)$	$R^2$	0.97	0.95	0.93	0.96	0.95
		$n$	0.57	0.34	0.41	0.34	0.33
		$\ln k$	-4.39	-3.16	-3.27	-2.83	-2.64

#### 4. Conclusions

The leaching rate of Al and Fe on the optimum acid concentration of different acids was shown that the iron removal rate of iron has no significant difference but the leaching rate of Al was 7.70, 12.68 and 4.25% using HCl, H<sub>2</sub>SO<sub>4</sub> and C<sub>2</sub>H<sub>2</sub>O<sub>4</sub>, the leaching rate of Al was maximal using H<sub>2</sub>SO<sub>4</sub> and minimum using C<sub>2</sub>H<sub>2</sub>O<sub>4</sub>, the results indicated that C<sub>2</sub>H<sub>2</sub>O<sub>4</sub> could protect the kaolin structure compared with HCl and H<sub>2</sub>SO<sub>4</sub>.

The optimal removal rate of iron reaches 29.09% (the content of Fe<sub>2</sub>O<sub>3</sub> decreased from 0.55 to 0.39%) under the conditions of 100 °C, 0.4 M C<sub>2</sub>H<sub>2</sub>O<sub>4</sub>, and L/S equal to 4 cm<sup>3</sup>/g for 120 min.

Kinetics analysis of removal rate of iron from coal-series kaolin showed that the leaching process was successfully described by the Avrami model and mainly controlled by internal diffusion control of shrinking core model. The Avrami model apparent activation energy was 18.46 kJ/mol. During the leaching of iron from coal-series kaolinite, oxalic acid first reacts with the surface of iron impurity particles to form a complex, and the reaction proceeds to the interior of the particles as the reaction time increases. The experimental results were consistent with the internal diffusion control of shrinking core model, improving acid concentration and leaching temperature to realize a high-efficiency removal of iron from coal-series kaolinite.

## Acknowledgements

This work was financially supported by “National Natural Science Foundation of China” (No. 51904121), “Science and Technology Research Project of Education Department of Jiangxi Province” (No: GJJ180476), “Science Foundation for Doctors of Jiangxi University of Science and Technology” (No: jxxjbs18056) and Innovation and Entrepreneurship Training Programme for university students (No: DC2019-007).

## References

- AMBIKADEVI, V.R., LALITHAMBIKA, M., 2000. *Effect of organic acids on ferric iron removal from iron-stained kaolinite*. Appl. Clay Sci. 16(3), 133-145.
- GUO, M.R., LIN, Y.M., XU, X.P., CHEN, Z.L., 2010. *Bioleaching of iron from kaolin using Fe(III)-reducing bacteria with various carbon nitrogen sources*. Appl. Clay Sci. 48(3), 379-383.
- HUANG, T., LEI, S.M., LIU, Y.Y., LI, B., 2019. *Optimization for the COD reduction and thermodynamics research of coal-series kaolin*. Environ Earth Sci. 78(12), 363.
- LEVENSPIEL, O., 1972. *Chemical Reaction Engineering*. Wiley, New York, 361-371.
- LIN M., LIU Y. Y., LEI S.M., YE Z., PEI Z.Y., LI B., 2018. *High-efficiency extraction of Al from coal-series kaolinite and its kinetics by calcination and pressure acid leaching*. Appl. Clay Sci, 161, 215-224.
- MARTINEZ-LUEVANOS, A., RODRIGUEZ-DELGADO, M.G., URIBE-SALAS, A., CARRILLO-PEDROZA, E.R., OSUNA-ALARCON, J.G., 2011 *Leaching kinetics of iron from low grade kaolin by oxalic acid solutions*. Appl. Clay Sci. 51(4), 473-477.
- SOKIĆ M.D., MARKOVIĆ B., ZIVKOVIĆ D., 2009. *Kinetics of chalcocopyrite leaching by sodium nitrate in sulphuric acid*. Hydrometallurgy. 95(3-4), 273-279.
- TUNÇ, M., KOCAKERİM, M.M., ÖZKAN, K., 2007. *Dissolution of colemanite in (NH<sub>4</sub>)<sub>2</sub>SO<sub>4</sub> solutions*. Korean J. Chem. Eng. 24(1), 55-59.
- QUEROL, X., IZQUIERDO, M., MONFORT, E., ALVAREZ, E., FONT, O., MORENO, T., ALASTUEY, A., ZHUANG, X., LU, W., WANG, Y., 2008. *Environmental characterization of burnt coal gangue banks at Yangquan, Shanxi Province, China*. Int. J. Coal Geol. 75(2), 93-104.
- VEGLIO, F., PAGLIARINI, A., TORO, L., 1993. *Factorial experiments for the development of a kaolin bleaching process*. Int. J. Miner. Process. 39(39), 87-99.
- XIA, G.H., LU, M., SU, X.L., ZHAO, X.D., 2012. *Iron removal from kaolin using thiourea assisted by ultrasonic wave*. Ultrason. Sonochem. 19(1), 38-42.
- YU, M.M., JIANG, X.Q., MEI, G.J., CHEN, X.D., 2017. *Leaching kinetic study of Y and Eu from waste phosphors using hydrochloric acid solution containing hydrogen peroxide*. Physicochem. Probl. Mineral Proc. 54(2), 238-248.
- ZHU, P.W., ZENG, W.Q., XU, X. L., CHENG, L.M., JIANG, X., SHI, Z.L., 2014. *Influence of acid leaching and calcination on iron removal of coal kaolin*. Int. J. Min. Met. Mater. 21(4), 317-325.